Journal of Alloys and Compounds 750 (2018) 669–676

Contents lists available at ScienceDirect

Journal of Alloys and Compounds

journal homepage: http://www.elsevier.com/locate/jalcom

High-temperature order-disorder phase transition in Fe-18Ga alloy evaluated by internal friction method

Meng Sun [a, b], Xianping Wang [a, *], Le Wang [a, b], Hui Wang [c, **], Weibin Jiang [a], Wang Liu [a], Ting Hao [a], Rui Gao [a], Yunxia Gao [a], Tao Zhang [a], Li Wang [c], Qianfeng Fang [a], Changsong Liu [a]

[a] Key Laboratory of Materials Physics, Institute of Solid State Physics, Chinese Academy of Sciences, Hefei 230031, PR China
[b] Department of Materials Science and Engineering, University of Science and Technology of China, Hefei 230026, PR China
[c] Science and Technology on Reactor Fuel and Materials Laboratory, Nuclear Power Institute of China, Chengdu, Sichuan, 610041, PR China

ARTICLE INFO

Article history:
Received 28 December 2017
Received in revised form
4 April 2018
Accepted 6 April 2018
Available online 7 April 2018

Keywords:
High damping alloy
Internal friction
Phase transition
Order-disorder
Magnetostriction

ABSTRACT

The structure, internal friction (IF) behavior, resistivity and magnetostriction property of Fe-18Ga alloy were systematically analyzed in this investigation. In the IF spectra of Fe-18Ga alloy covered from room temperature (RT) to 800 °C, a prominent IF peak (labeled as P_{tr} peak) was observed in the high temperature range 530 °C–690 °C besides the reported IF peak related with grain boundary relaxation in the moderate temperature range 400 °C–530 °C. The peak position of P_{tr} peak hardly changes with measuring frequency, implying that its mechanism is most possibly related with phase transition. Considering from the wide peak shape, P_{tr} peak can be decomposed into two components: the lower temperature P_{tr1} peak located around 530 °C–605 °C and the higher temperature P_{tr2} peak located around 605 °C–690 °C. Combined with calculated phase diagram, resistivity and magnetostriction analysis, the mechanism of P_{tr} peak was suggested to originate from the order-disorder phase transition related with Ga atom distribution in Fe-18Ga alloy: P_{tr1} peak was ascribed to $D0_3 \rightarrow B2$ transition and P_{tr2} peak was ascribed to $B2 \rightarrow A2$ transition, respectively.

1. Introduction

Fe-Ga based alloys, as novel magnetostrictive materials, have become the focus of attention due to their excellent comprehensive properties in the past two decades [1–3]. These properties include small brittleness, high mechanical strength, lower cost, good thermal stability and high magnetostriction coefficient [4]. Fe-Ga based alloys, similar to Fe-Al, Fe-Mo and Fe-Cr based ferromagnetic materials, also exhibit high-damping property [5–7]. The main damping mechanism is associated with magnetomechanical damping, that is: when the external stress is applied, the internal magnetic domain of the material will slip and rotate. The slip and rotation of the magnetic domain will consume energy and therefore exhibits high damping effect [8]. The previous studies revealed that the magnetostriction coefficient of polycrystalline Fe-Ga binary alloy was closely related to Ga content, and it has two maxima of magnetostricition (λ_s) at 17–19 and 27 at% Ga [9]. According to Smith and Birchak's theory [10], maximal hysteretic internal friction (IF) (labeled as Q^{-1}_{max}) is proportional to magnetostriction coefficient λ_s of ferromagnetic materials: $Q^{-1}_{max} \sim \lambda_s$. Especially for Fe-18Ga and Fe-27Ga alloys, the maximum IF (Q^{-1}_{max}) can be as high as 0.04 and 0.06 respectively owing to their high magnetostricition properties [11]. Therefore, Fe-Ga based alloys may be good candidates as high damping materials, which have wide application in decreasing vibration, noise reduction and other related fields.

In the aspect of crystal structure, Fe-Ga based alloys exhibit relatively complex multi-phase structures. Under certain conditions, a variety of phase structures, such as A2, B2, $D0_3$, $D0_{19}$ and $L1_2$ as well, appear in Fe-Ga alloy with Ga concentration between 15 and 30 at.%. Among these phases, A2 (sp. gr. Im3m) belongs to bcc structure with Fe atom randomly replaced by Ga atoms, B2 (sp. gr. Pm3 m) has a CsCl-type structure with Ga atom staying at the body-centered sites, while $D0_3$ (sp. gr. Fm3m) has a BiF_3-type structure with a unit cell lattice parameter extending about twice that of bcc

* Corresponding author.
** Corresponding author.
E-mail addresses: xpwang@issp.ac.cn (X. Wang), qinghe5525@163.com (H. Wang).

https://doi.org/10.1016/j.jallcom.2018.04.062
0925-8388/

iron [1]. The formation of equilibrium fcc-based $L1_2$ ordered phase in Fe-Ga binary alloys below 650 °C is rather slow in nature. So in most cases, the phase transition in Fe-Ga alloy develops in accordance with the metastable diagram shown in Fig. 1a [1], and is expected to an equilibrium of A2 and $D0_3$ phases at room temperature (RT).

It is necessary to point out that the formation of transient nonstoichiometric B2 phase in Fe-Ga alloy possibly takes place prior to $D0_3$ phase in terms of theory simulation [12]. For example, related simulation results show that A2 phase in Fe-18 at% Ga alloy can decay as A2→B2→$D0_3$ gradually, accompanied by the formation of B2 nanoprecipitates with the gain size from 3 to 10 nm at the intermediate stage, as shown in Fig. 1b [12]. This result is not accordance with the existing experimental phase diagram shown in Fig. 1a, in which the single A2 phase at high temperature(~550 °C) directly transforms into a mixture of A2 and $D0_3$ phase, and the intermediate B2 phase isn't formed in the Fe-Ga system if Ga ratio is less than 22%. More importantly, calculated results demonstrated that the nonstoichiometric B2 phase could be responsible for the high magnetostriction coefficient in Fe-Ga alloys. Thus, how to explore B2 phase predicted by theory simulation as well as the existence temperature range is very important owing to the key contribution of the nonstoichiometric B2 phase in high magnetostricition properties.

It is well known that the IF behavior is particularly sensitive to phase transition and defects in solid materials. The complex phase structures as well as structure evolution in Fe-Ga alloys generally produce rich IF phenomena, and the related analysis and research based on IF phenomena and mechanism can thus provide important information for designing and developing Fe-Ga based high damping materials owing to its excellent magnetostricition effect. M. Ishimoto et al. studied the effect of temperature on IF behavior of Fe-17 at% Ga alloy [13], and found that there was a high-damping plateau over the temperature range -190-300 °C, where the damping value can be up to 10^{-2}. Golovin et al. carefully studied the IF behavior of the quenched Fe-19 at% Ga alloy, and a series of IF peaks were reported in temperature spectra [11,14,15]. Besides the high damping plateau below 300 °C, a phase transition IF peak near 450 °C caused by $D0_3$→$L1_2$ transition and a relaxational-type IF peak related to grain boundary near 500 °C were also observed by Golovin et al. [14]. It worth noting that a weak frequency independent IF peak was observed at around 490 °C, but its mechanism has not been well explained due to the peak temperature close to $D0_3$ to A2 phase transition and the Curie temperature of $D0_3$ ordered phase [15–17]. Though Fe-Ga alloy, as a new kind of high damping material, has attracted more attention in recent years, the investigated temperature regime is generally concentrated in RT to 600 °C, and the IF behaviors at higher temperature range, which play an important role related with their good magnetostriction property, have not been reported till now.

In this paper, the IF behavior of Fe-18Ga alloy through a wide temperature range (RT~800 °C) was investigated. Besides the reported IF peaks in the lower temperature range (RT~530 °C), two prominent IF peaks were observed in the higher temperature range (530–690 °C). The mechanism of the two peaks was suggested to originate from the order-disorder transition related with Ga distribution in Fe-18Ga alloy: from the long-range ordered $D0_3$ phase to the transient B2 phase, and further transform into disordered A2 phase with increasing temperature. The approximate temperature range of B2 phase in Fe-18Ga alloy was firstly determined by IF method. The obtained results are not only helpful to understand the enhancement mechanism of magnetostriction in Fe-Ga alloy caused by atomic ordering, but is also advantageous to design and develop high damping Fe-Ga based alloy with excellent performance.

2. Experimental technique

The ingots of Fe-18Ga alloy were produced in a vacuum arc melting furnace using pure Fe (99.99 wt%) and pure Ga (99.99 wt%). The actual concentrations of Ga were determined to be 18.3 ± 0.2 mol% by high resolution inductive coupled plasma emission spectrometer (ICP) and energy-dispersive spectroscopy (EDS). The measured samples were cut from the ingots using a cutting machine. Besides preserving original as-cast sample (As-cast), the Fe-18Ga samples were subjected to two different heat treatments: the samples were annealed in the Ar atmosphere for 1 h at 1000 °C at first, then water quenched (Wq^{o}_{1000C}) or (ii) furnace cooling (Fc^{o}_{1000C}).

Structural characterization was performed with an X-ray diffraction meter (XRD, X'Pert Pro MPD) and a transmission electron microscope (TEM, JEM-2000FX). For convenience of comparison, all XRD samples were mechanically polished as the same size ($10 \times 10 \times 2\ mm^3$). The scanning range was 20–120° for 2θ at a step size of 0.033°/s. In order to resolve the overlapping peaks of different phases, high resolution scans around 2θ = 81.5° were

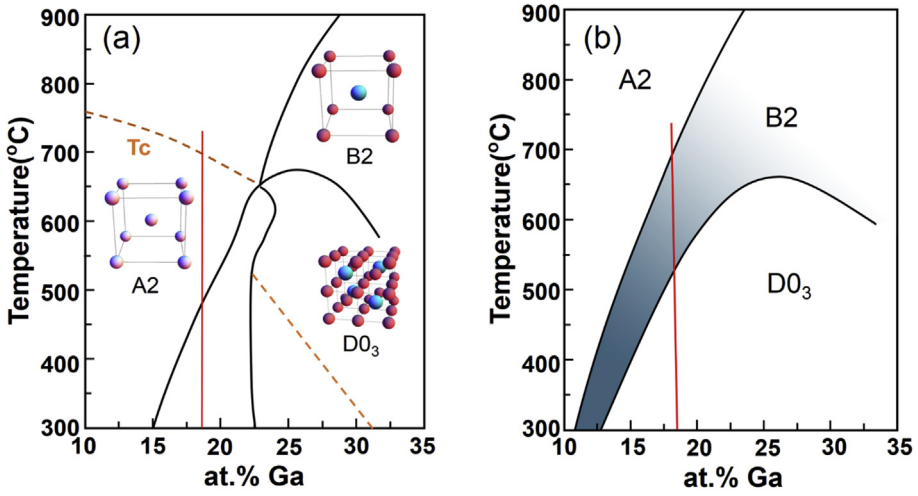

Fig. 1. (a) Metastable phase diagram of Fe-Ga alloy [1]; (b) Calculated phase diagram of Fe–Ga alloy [12].

taken using a smaller step size of 0.008°/s. TEM samples were prepared by a TENUPOL 5 twin-jet polisher using 7% HNO_3 + 93% CH_3CH_2OH (volume fraction) as electrolyte at −30 °C.

The IF behavior of Fe-18Ga alloy was measured by a computer-controlled automatic inverted torsion pendulum with the force-vibration mode, in which different frequencies (1–5 Hz) were carried out in one measurement run with a heating rate of 2 K/min over a temperature range from RT to 800 °C. The sample size in the IF measurement is about $2 \times 1 \times 23\ mm^3$. The maximum torsion strain amplitude was kept at 3×10^{-5} in all measurements. The whole measuring process was carried out in vacuum to avoid oxidation at high temperature.

The order-disorder transition of Fe-Ga alloy is often accompanied by an anomalous change in the resistivity-temperature curve (ρ-T curve). The resistance measurement in this investigation was measured by a four-electrode method with a constant current of 100 mA. Both resistance and IF measurements were carried out simultaneously in a same apparatus to ensure the accuracy and consistency of temperature. Through the resistance measurement, the ρ-T curve was derived by $\rho = RS/L$, where the sectional area S is about 2 mm^2, and the sample length L is about 23 mm.

Magnetic behavior of the investigated Fe-18Ga samples treated at different temperature was investigated at RT with magnetic field up to 2000 Oe. The RT magnetostriction was measured by the Quantum Design's physical property measurement system (PPMS-9), and the applied magnetic field is paralleled to the sample plane. The strain gauge bonded longitudinally on the Fe-18Ga samples was used to determine the magnetostrictive coefficient, and the corresponding noise level is less than 2×10^{-6}.

3. Results

3.1. XRD characterization

Fig. 2a shows the XRD profiles for the Fe-18Ga samples at three different heat treatment states of As-cast, Wq^{o}_{1000C}, and Fc^{o}_{1000C}, respectively. The basic diffraction peaks are (110), (200), (211), (220), and (310), respectively, and all samples exhibit the similar cubic structure as α-Fe. The unit cell parameters of the samples are about 2.883 Å deduced by MDJ Jade full-spectrum fitting, which is slightly larger than that of α-Fe (2.863 Å). The main reason is that the solution of larger radius Ga atom (0.140 nm) in lattice in comparison with Fe atom (0.124 nm), which results in an increase of unit cell parameter. To further explore the tiny difference caused by heat treatment, Fig. 2b–d shows the fine diffraction spectra near $2\theta = 81.5°$ for the As-cast, Wq^{o}_{1000C}, and Fc^{o}_{1000C} samples, respectively. It can be seen from Fig. 2b–d that small diffraction peak splitting is observed at a slightly higher angle ($2\theta = 81.8°$) in the Fc^{o}_{1000C} sample besides the main diffraction peak (211) of A2 phase. The slight splitting actually corresponds to the diffraction peak of $D0_3$ phase [9]. The coexistence of A2 and $D0_3$ phases in Fe-18Ga alloy is in agreement with the reported results in Refs. [9,15], and the distribution of Ga in Fe-Ga alloys had been determined as long-range disorder by T. A. Lograsso et al. [18,19].

It is known that the diffraction intensity of XRD peak is closely related with the phase content in muti-phase materials. The slight splitting of (211) peak for the Fc^{o}_{1000C} sample indicates that the volume fraction of $D0_3$ phase in the two-phase Fe-18Ga alloy is actually much lower than that of A2 phase. Further, according to the

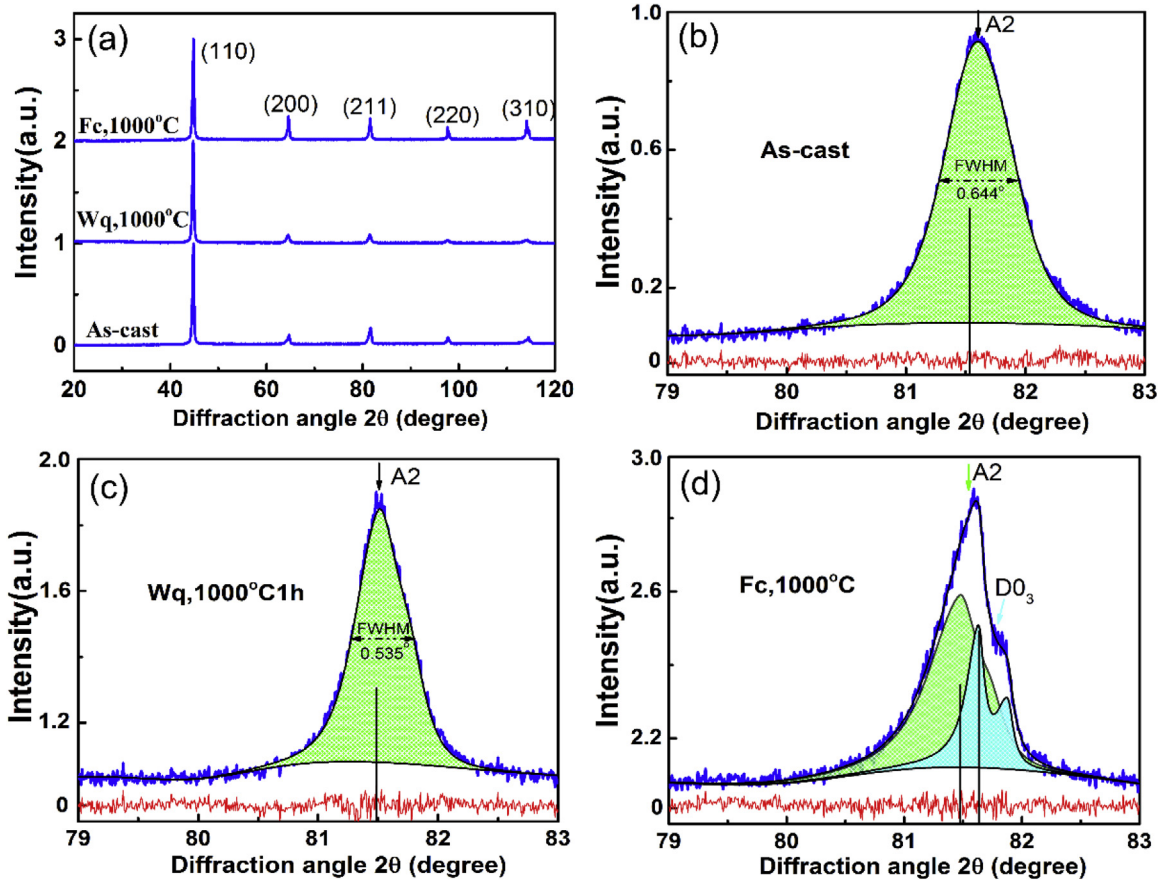

Fig. 2. (a) X-ray diffraction spectra for the Fe-18Ga samples at different heat treatment states; (b–d) high resolution scans for (211) reflection peak in the vicinity of 79°–83°, and the peak has been fitted using a pseudo-voight profile.

similarity in the atomic scattering factors among different Fe-Ga phases, the volume fraction of different phases in the Fc^{o}_{1000C} sample can be evaluated by diffraction intensity, as shown in Fig. 2d. The area analysis evaluated by MDJ Jade fitting reveals that the volume fraction of A2 phase and $D0_3$ phase is about 70.81% and 29.19%, respectively. After making precise comparison of XRD profiles between in As-cast and Wq^{o}_{1000C} samples, the half maximum (FWHM) of the (211) line for the As-cast sample (0.644°) is found to be slightly wider than that of the Wq^{o}_{1000C} sample (0.535°). This result implies that the As-cast sample most possibly contain a little amount of $D0_3$ phase, rather than single A2 phase, owing to the slower cooling rate in the air than that in the water quenched condition, and further studies will be discussed in detail in the following IF measurement.

3.2. IF measurement

Fig. 3 shows the variation of IF and relative modulus (M) versus temperature for an As-cast Fe-18Ga sample at three different vibration frequencies of 1, 3 and 5 Hz, respectively, and the heating rate is maintained at 2 K/min. It can be seen from Fig. 3a that a high damping plateau with IF value of 0.012 is observed over the temperature range of RT to 200 °C, and then the IF value decreases rapidly to about 0.003 around 310 °C. Further increasing temperature to 800 °C, two pronounced IF peaks (labeled as P_1 at lower temperature and P_{tr} at higher temperature) are observed. In the temperature regime of IF peaks, obvious variation of relative modulus is observed.

The high damping plateau over the temperature range from RT to 200 °C had been suggested to be related to two main damping mechanisms: non-magnetic damping (dislocation, grain boundaries, and point defects) and magneto-mechanical damping [16]. The magneto-mechanical damping behavior in ferromagnetic materials originates from stress-driven irreversible movement of the magnetic domain walls [8]. With increasing temperature, the magnetism of ferromagnetic alloy gradually decreases, and therefore leads to the decrease of damping related to magnetic domain wall movement in Fe-18Ga alloy. For P_1 peak, the peak center is located at 467 °C at 1 Hz, and the peak position shifts toward a higher temperature with increasing frequency, which is a typical characteristic of a relaxation IF peak. The relaxation mechanism of P_1 peak was mainly ascribed to grain boundary relaxation [11]. As for P_{tr} peak at higher temperature range (530 °C–690 °C), the peak position hardly changed with increasing measurement frequency, while the net peak height ($\Delta Q_{P_{tr}}^{-1}$) after subtracting IF background decreases with increasing frequency (See the inset in Fig. 3). Both peak position and peak height exhibit typical characteristics of a phase transition. In Fe-Ga alloys, the observed P_{tr} peak was not reported in the previous literature, and the corresponding mechanisms will be further discussed based on double subpeak structure in the following sections.

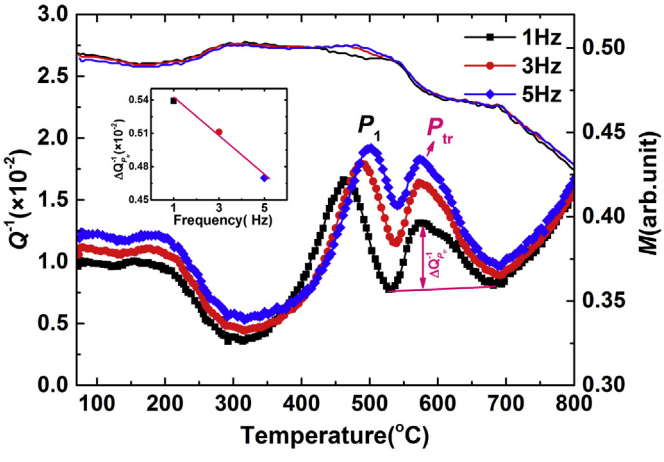

Fig. 3. Temperature dependence of the IF (Q^{-1}) and the relative modulus (M) for an As-cast Fe-18Ga sample at three different frequencies of 1, 3, and 5 Hz with a heating rate of 2 K/min. Insert: the variation of peak height ΔQ^{-1} versus frequency.

3.3. Resistivity measurement

Fig. 4a–c shows the temperature dependence of IF, resistivity, and resistivity difference ($\frac{d\rho}{dT}$) over the temperature range of 500–730 °C for the As-cast Fe-18Ga alloy sample. Both measurements are carried out simultaneously at a same heating rate of 2 K/min to ensure the consistency of temperature. It can be seen from Fig. 4a that an obvious and broad peak is observed in the investigated temperature range. Further considering the peak shape, P_{tr} peak can be decomposed into two subpeaks: the lower temperature component located around 530 °C–605 °C is labeled as P_{tr1} peak and the higher temperature component located around 605 °C–690 °C is labeled as P_{tr2} peak.

The resistivity result is shown in Fig. 4b, in which the resistance gradually increases from 0.64 Ωm to about 0.68 Ωm at first and then saturate at this value in the investigated temperature regime. In the temperature range of IF peak from 530 °C to 690 °C, the resistivity curve varies smoothly and no abrupt change is detected. To further explore the relationship between resistivity and temperature, the resistivity differential curve ($\frac{d\rho}{dT}$) versus temperature was given, as shown in Fig. 4c. Two obvious transition zones (labeled as A and B) are observed, which correspond well to P_{tr1} peak at lower temperature and P_{tr2} peak at higher temperature, respectively.

Combined with the metastable diagram of Fe-Ga binary alloy shown in Fig. 1, there is a $D0_3 \rightarrow A2$ phase transition around 500 °C at 18 at.% Ga, from an ordered state of Ga atom distribution to disordered state. This phase transition most possibly results in the variation of resistivity as well as the transition in differential curve. Considering conduction in metals, the resistance is caused by the scattering of electrons in the alloy. When the electrons move in the disordered solid solution, the probability of electrons scattering is

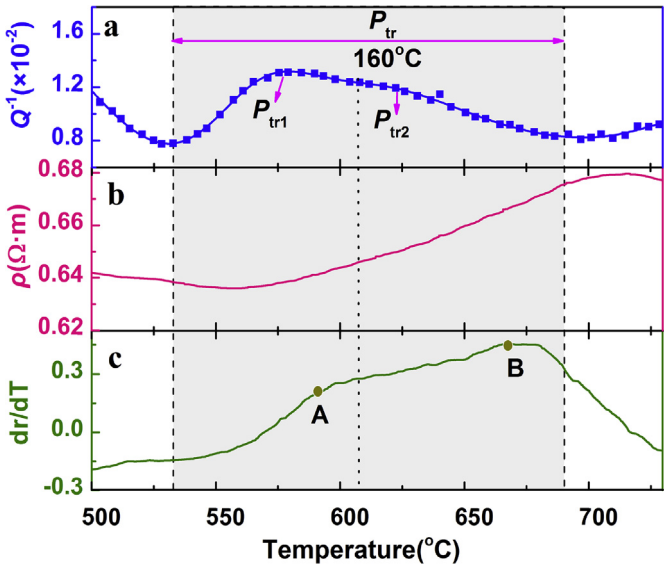

Fig. 4. IF(a), resistivity (b), and resistivity differential ($\frac{d\rho}{dT}$) (c) versus temperature for the As-cast Fe-18Gaalloy with a heating rate of 2 K/min.

higher than that in the ordered solid solution. Thus, the average free path of electrons in the disordered solid solution is shorter, leading to higher resistivity than that in more ordered atomic structure, as shown in Fig. 4b.

The mechanism of P_{tr} peak should be also ascribed to the order-disorder phase transition related with Ga distribution owing to its typical phase transition characteristic. Moreover, the two sub-component structures show that this phase transition could be quite complex, but not a single structural phase process. The complexity of the phase transition can be also confirmed by the two-inflection zones in resistivity differential curve shown in Fig. 4c. The detailed IF mechanism related the phase transition will be further analyzed in the following discussion.

4. Discussion

4.1. Relaxation parameter of P_1 peak

According to the experimental results shown in Fig. 3, P_1 peak exhibits typical relaxation characteristic, and the mechanism is ascribed to grain boundary relaxation [11]. The IF curve related with relaxation mechanism, such as point defects and grain boundary, can well fitted by one or more Debye peak and an IF background Q_B^{-1} based on a non-linear fitting method [20]. Here, Q_B^{-1} can be described as $Q_B^{-1} = B + Ce^{-Q_b/kT}$, where both B and C are frequency-dependent constants, Q_b is an apparent activation energy. In Fig. 5a, the nonlinear fitting results of P_1 peak based on one Debye peak are presented, where the symbols represent the data points at different frequencies, the solid line is the fitting peak, and the gray dash line is the fitting background. Thus the peak temperature T_p at different measurement frequencies can be precisely determined.

As known that for a relaxation process related with thermal activation, the IF peak occurs at the following condition [21]:

$$\omega\tau = \omega\tau_0 \exp\left(\frac{H}{kT_P}\right) = 1,$$

where τ is the relaxation time, τ_0 is the pre-exponential factor, ω is the circular frequency ($=2\pi f$, f is the measuring frequency), H is the activation energy, k is Boltzmann constant, and T_P is peak temperature of IF peak. From the relationship between the logarithm of circular frequency ω and the reciprocal of peak temperature ($1/T_p$), the activation energy H and pre-exponential factor τ_0 can be evaluated, as shown in Fig. 5b, where the Arrhenius plot of P_1 peak for as-cast Fe-18Ga alloy is given. In terms of such linear fitting, the relaxation activation energy H and the pre-exponential factor τ_0 are determined as 2.3 eV and 10^{-17}s, respectively. The obtained parameters related with grain boundary are well consistent with the reported results ($H = 2.4$ eV, $\tau_0 = 10^{-17}$s) in similar Fe-Ga system by Golovin et al. [16].

4.2. Mechanism of P_{tr} peak

In order to clarify the factors that affect the formation of P_{tr} peak in Fe-18Ga alloy, Fig. 6 gives the IF curves around peak temperature range (520 °C–720 °C) after different heat treatments ($Fc^{o}_{1000C,}$ As-cast, and Wq^{o}_{1000C}). During the whole experiments, the measurement frequency, strain amplitude and heating rate were 1 Hz, 3×10^{-5} and 2 K/min, respectively. It is clear that from Fig. 6 the peak position of P_{tr1} peak remains unchanged with different heat treatment (Fc^{o}_{1000C}, As-cast, and Wq^{o}_{1000C}), while the peak height decreases successively, and trend of P_{tr2} peak is similar to that of P_{tr1} peak. The peak temperature of P_{tr1} and P_{tr2} peak is independent of the frequency, implying that they should be caused by phase transition.

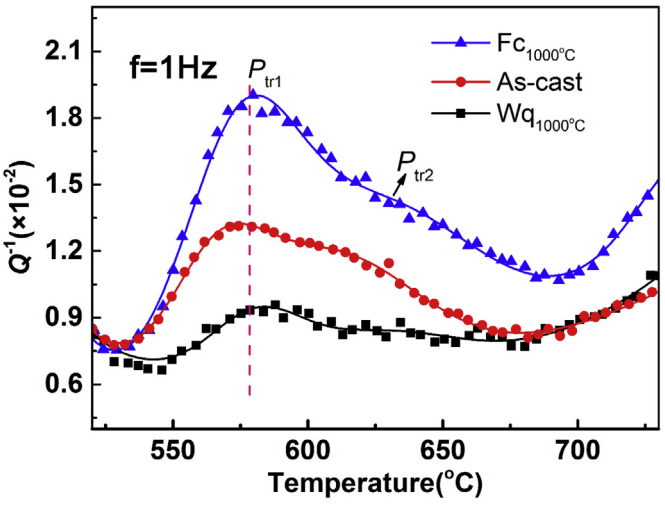

Fig. 6. Temperature dependence of IF curves for the Fe-18Ga alloys under different heat treatments ($Fc^{o}_{1000C,}$ As-cast, and Wq^{o}_{1000C}) at 1 Hz.

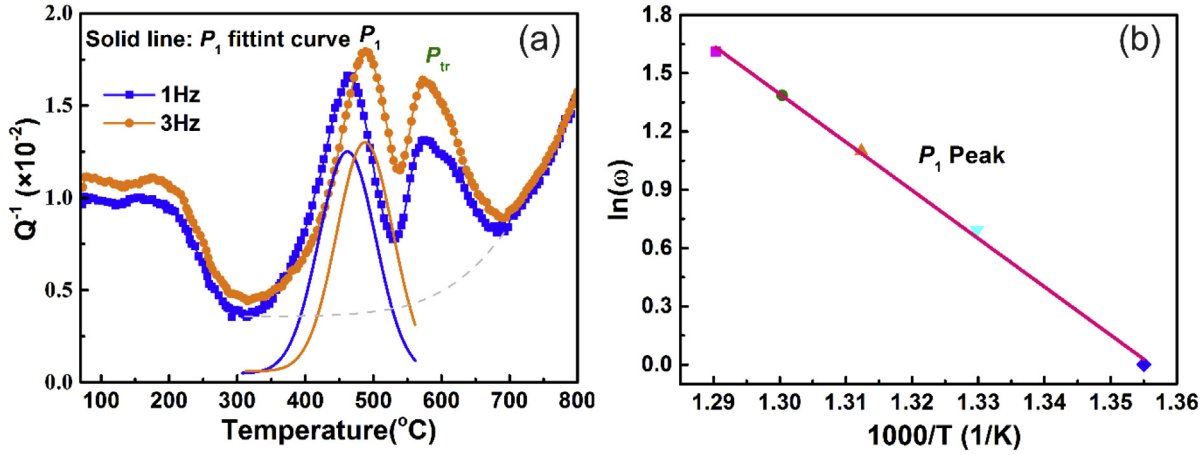

Fig. 5. (a)Temperature dependence of IF (Q^{-1}) for an As-cast Fe-18Ga sample measured at 1 and 3 Hz. Solid lines are the fitting curves of P_1 peak, and the dash line is fitting background. (b) Arrhenius plot of P_1 peak. The relaxation activation energy was deduced as 2.3 eV by calculating the slope of the fitting line.

According to the XRD results above, the quenched Fe-18Ga sample from high temperature exhibits single A2 phase, and the formation of $D0_3$ ordered phase is suppressed. On the contrary, a very small amount of $D0_3$ phase precipitates in A2 parent phase in the As-cast sample when the alloy is cooled slowly. For the furnace cooled sample, more $D0_3$ precipitate is observed owing to the slowest cooling rate, as evidenced by the splitting of (211) diffraction line. In terms of phase diagrams of Fe-Ga alloy as well as resistivity measurement, the mechanism of P_{tr} peak is ascribed to the order-disorder phase transition related $D0_3$ phase. The basic IF theory predicted that the intensity of IF peak caused by phase transition is proportional to the transformation amount of materials [21]. The consistence between the intensity of IF peak and $D0_3$ amount confirms that P_{tr} peak is most possibly caused by the phase transition related to $D0_3$ phase. But the two subcomponent structures for P_{tr} peak implies that the phase transition should be not only ascribed to single $D0_3 \rightarrow A2$ transformation, but should contain two structural transition processes related with Ga atom distribution.

According to simulated phase diagram shown in Fig. 1b, the phase transition doesn't occur simply from $D0_3$ to A2 in fact, but from $D0_3$ to B2 at first and then from B2 to A2 phase with increasing temperature, which covers a relatively wide temperature range in the whole phase transition. Generally, it is quite difficult to explore B2 phase in A2 matrix owing to the small difference in crystal structure between A2 and B2 phase by structural analysis.

In Fig. 7a, the RT magnetostriction results are presented for the five Fe-18Ga samples. These samples were annealed for 30 min at 450, 560, 620, 680, and 750 °C at first, and then water quenched, respectively. The applied magnetic field is from zero up to a maximum value of 2000 Oe. As can be seen from Fig. 7a, the magnetostriction coefficient (λ_s) rapidly increases at first and then gradually saturates for all measured samples when the applied magnetic field reaches and exceed about 800 Oe. The saturated magnetostriction coefficient varies substantially with annealing temperature, and a maximum value of 112 ppm is found for the Fe-18Ga sample quenched at 620 °C (labeled as Wq^{0}_{620C}). This value is obviously larger than that of other samples (60–80 ppm). T. Y. Ma et al. also found that the magnetostrictive coefficient of Fe-19Ga alloy quenched near the phase transition zone was about 71.4% higher than that of the sample quenched from higher temperature (1000 °C) [22]. Such magnetostriction results may confirm the existence of transient B2 phase in intermediate temperature region, as predicted by theory simulation result [12].

To understand the enhancement of magnetostriction, Fig. 7b gives the HRTEM image of the uniform A2 field of the Wq^{0}_{620C} sample. In the bright area, the FFT image of the A2 field exhibits (022) and (202) spots along the [111] direction, as shown in Fig. 7c, which corresponds to the diffraction pattern of A2 phase. In the bright area, the FFT image of the A2 field exhibits (110) and (112) spots as shown in Fig. 7d, which corresponds to the diffraction pattern of the distorted B2 phase [23]. For paramagnetic B2 phase, it cannot be responsible for the good magnetostriction at RT in Fe-Ga alloys. Boisse J et al. studied the structural transformations of Fe-Ga alloy by using computer modeling of the atomic-scale ordering and clustering in the atomic density field approximation [12], and suggested that the cubic B2 phase at higher temperature would be distorted into a tetragonal B2 phase (i.e. $L1_0$ phase) by a cubic to tetragonal martensitic transformation in cooling process. The tetragonal $L1_0$ phase belongs to ferromagnetic phase at RT, and the reorientation of tetragonal phase under a magnetic field thus exhibits high magnetostriction [12,24,25]. Based on the theoretical results above, the enhancement of magnetostriction shown in Fig. 7a is speculatively ascribed to the cubic→tetragonal transition in Fe-18Ga alloy at present. It is necessary to point out that to clearly understand its mechanism, more direct experimental evidences are still needed in the future research.

From the resistivity and magnetostriction results, the mechanisms of P_{tr} peak is suggested to be related to the order-disorder phase transition, i.e. long-range ordered $D0_3$ phase to the intermediate B2 phase and further transformation into the completely disordered A2 phase. It is necessary to point out that only the $D0_3$ phase contained in the A2 matrix participates in the phase transition owing to the existence of A2 phase in the whole temperature range. Moreover, according to the two component configuration of P_{tr} peak as well as to the calculated phase diagram shown in Fig. 1b, the mechanism can be explained by a two-phase model. P_{tr1} peak at lower temperature and P_{tr2} peak at higher temperature are ascribed to $D0_3 \rightarrow B2$ transition and $B2 \rightarrow A2$ transition, respectively.

The schematic IF diagram related the phase transition is presented in Fig. 8. Noting that the phase transition of P_{tr} peak actually covers a wide temperature range from 530 °C to 690 °C, which means that the transition process related with Ga distribution should be quite slow. As known that IF in a phase transition process is closely related to transformation amount. In the initial stage (~530°C-560 °C), the phase transition from $D0_3$ to B2 phase starts to initiate, which corresponds to the nucleation and growth of the new B2 phase. With the increase of the temperature, the $D0_3$

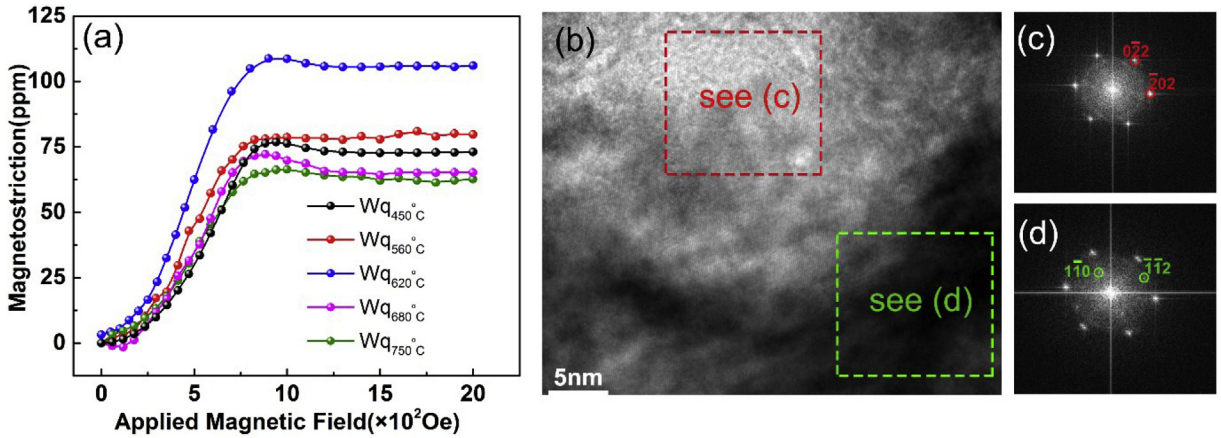

Fig. 7. (a) Magnetostriction curves for Fe-18Ga samples quenched at different temperatures (560 °C,560 °C, 620 °C, 680 °C and 750 °C); (b) An HRTEM image of the uniform A2 field of Fe-18Ga sample quenched at 620 °C; (c) an FFT image of the bright area marked by the red line; (d) an FFT image of the dark area by the green line. (For interpretation of the references to colour in this figure legend, the reader is referred to the Web version of this article.)

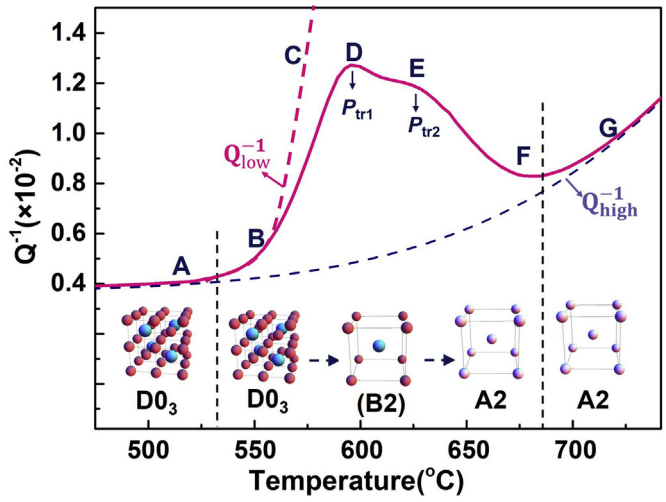

Fig. 8. Phase transition schematic diagram of P_{tr} peak in Fe-18Ga alloy based on two-phase model.

gradually transforms into the B2 phase. Further at the top point of P_{tr1} peak(~580 °C), the phase transformation rate from $D0_3$ to B2 phase reaches up to maximum according to the proportion relation between IF value and phase transition rate. The occurrence of such phase transition also leads to the remarkable increase of resistivity, as shown in Fig. 4. Continuously increasing experimental temperature, the IF gradually decreases, implying the drop of transformation rate from $D0_3$ to B2 phase. As suggested above, P_{tr2} peak centered at 625 °C is ascribed to B2 to A2 phase transition, which is finally ended at about 690 °C. The center peak position located at 625 °C corresponds to the maximum transformation rate from B2 to A2 phase. In the intermediate temperature region from 580 °C to 625 °C, both two-phase transition processes possibly occur simultaneously, which corresponds to the gradual end of $D0_3$ to B2 phase transition and the beginning of B_2 to A2 phase transition. It should be pointed out that our interpretation based on IF result only describes the phase transition steps related with Ga distribution in Fe-18Ga alloy, the mechanism description on atomic scale still requires further experimental investigation.

5. Conclusions

The IF behaviors of Fe-18Ga alloy with different heat treatment were carefully analyzed by a computer controlled automatic inverted torsion pendulum under a temperature range of RT to 800 °C. Besides the high damping plateau over the temperature range from RT to 200 °C, two prominent IF peaks were observed, labeled as P_1 peak and P_{tr} peak, respectively. The lower temperature P_1 peak located around 467 °C at 1 Hz exhibits typical relaxation characteristic, and the mechanism is ascribed to the grain boundary relaxation. The corresponding relaxation activation energy H and the pre-exponential factor τ_0 are determined as 2.3 eV and 10^{-17}s, respectively. With regard to higher temperature P_{tr} peak covered a wide temperature range 530 °C–690 °C, it is actually composed of two components: the lower temperature P_{tr1} peak located around 530 °C–605 °C and the higher temperature P_{tr2} peak located around 605 °C–690 °C. The insensitivity of peak position with measuring frequency implies its mechanism is most possibly related to a phase transition. Combining the calculated phase diagram of Fe-Ga alloy as well as the resistivity and magnetostriction measurement results, it is proposed that the mechanism of P_{tr} peak originates from the order-disorder phase transition related with Ga distribution: P_{tr1} peak is ascribed to $D0_3 \rightarrow$B2 transition and P_{tr2} peak is ascribed to B2 → A2 transition, respectively. Our investigation also demonstrates that the existence of B2 phase in Fe-Ga matrix can enhance its magnetostriction coefficient, and the obtained results are not only helpful to understand the mechanism of magnetostriction, but also helpful to design and develop high damping Fe-Ga based alloy with better performance.

Acknowledgements

This work was financially supported by the National Natural Science Foundation of China (Grant Nos.51771181, 11775255, 11575231, 51771184) and the CASHIPS Director's fund (Grant No.YZJJ201703).

References

[1] O. Ikeda, R. Kainuma, I. Ohnuma, K. Fukamichi, K. Ishida, Phase equilibria and stability of ordered bcc phases in the Fe-rich portion of the Fe-Ga system, J. Alloys Compd. 347 (1) (2002) 198–205.
[2] N. Srisukhumbowornchai, S. Guruswamy, Large magnetostriction in directionally solidified FeGa and FeGaAl alloys, J. Appl. Phys. 90 (11) (2001) 5680–5688.
[3] A.E. Clark, J.B. Restorff, M. Wun-Fogle, T.A. Lograsso, D.L. Schlagel, Magnetostrictive properties of body-centered cubic Fe-Ga and Fe-Ga-Al alloys, IEEE Trans. Magn. 36 (5) (2000) 3238–3240.
[4] A.E. Clark, M. Wun-Fogle, J.B. Restorff, K.W. Dennis, T.A. Lograsso, R.W. McCallum, Temperature dependence of the magnetic anisotropy and magnetostriction of $Fe_{100-x}Ga_x$ (x= 8.6, 16.6, 28.5), J. Appl. Phys. 97 (10) (2005), 10M316.
[5] I.S. Golovin, H. Neuhäuser, A. Riviére, A. Strahl, Anelasticity of Fe–Al alloys, revisited, Intermetallics 12 (2) (2004) 125–150.
[6] H. Wang, H. Huang, X. Hong, C. Yin, Z. Huang, L. Chen, Research on low strain magnetic mechanical hysteresis damping performance of Fe–15Cr–3Mo–0.5 Si alloy, J. Alloys Compd. 622 (2015) 17–23.
[7] Y. Xu, X. Chen, On relationship between annealing treatment and magnetostriction behavior of Fe–16Cr–2.5Mo damping alloy, J. Alloys Compd. 582 (2014) 364–368.
[8] R.C. Frank, J.W. Ferman, Magnetomechanical damping in iron-silicon alloys, J. Appl. Phys. 36 (7) (1965) 2235–2242.
[9] T.A. Lograsso, E.M. Summers, Detection and quantification of $D0_3$ chemical order in Fe–Ga alloys using high resolution X-ray diffraction, Mater. Sci. Eng., A 416 (1) (2006) 240–245.
[10] G.W. Smith, J.R. Birchak, Internal stress distribution theory of magneto-mechanical yysteresisan extension to include effects of magnetic field and applied stress, J. Appl. Phys. 40 (13) (1969) 5174–5178.
[11] I.S. Golovin, V.V. Palacheva, V.Y. Zadorozhnyy, J. Zhu, H. Jiang, J. Cifre, T.A. Lograsso, Influence of composition and heat treatment on damping and magnetostrictive properties of Fe–18%(Ga+ Al) alloys, Acta Mater. 78 (2014) 93–102.
[12] J. Boisse, H. Zapolsky, A.G. Khachaturyan, Atomic-scale modeling of nanostructure formation in Fe–Ga alloys with giant magnetostriction: cascade ordering and decomposition, Acta Mater. 59 (7) (2011) 2656–2668.
[13] M. Ishimoto, H. Numakura, M. Wuttig, Magnetoelastic damping in Fe–Ga solid-solution alloys, Mater. Sci. Eng., A 442 (1) (2006) 195–198.
[14] I.S. Golovin, Anelasticity of Fe–Ga based alloys, Mater. Des. 88 (2015) 577–587.
[15] A.A. Emdadi, J. Cifre, O.Y. Dementeva, I.S. Golovin, Effect of heat treatment on ordering and functional properties of the Fe–19Ga alloy, J. Alloys Compd. 619 (2015) 58–65.
[16] I.S. Golovin, J. Cifre, Structural mechanisms of anelasticity in Fe–Ga-based alloys, J. Alloys Compd. 584 (2014) 322–326.
[17] S.A.E. Boyer, M. Gerland, A. Rivière, J. Cifre, V.V. Palacheva, A.V. Mikhaylovskaya, I.S. Golovin, Anelasticity of the Fe-Ga alloys in the range of Zener relaxation, J. Alloys Compd. 730 (2018) 424–433.
[18] T.A. Lograsso, A. R Ross, D. L Schlagel, A.E. Clark, M. Wun-Fogle, Structural transformations in quenched Fe–Ga alloys, J. Alloys Compd. 350 (1–2) (2003) 95–101.
[19] M. Huang, T.A. Lograsso, Short range ordering in Fe–Ge and Fe–Ga single crystals, Appl. Phys. Lett. 95 (17) (2009), 07B310.
[20] L.X. Yuan, Q.F. Fang, Nonlinear fitting of the internal friction data and its application on the bamboo grain boundary relaxation pure Al, Acta Met. Sinica 34 (1998) 1016–1020 (in Chinese).
[21] A.S. Nowick, B.S. Berry, Anelastic Relaxation in Crystalline Solids, Academic Press, New York, 1972.
[22] N. Rahman, J. Gou, X. Liu, T. Ma, M. Yan, Enhanced magnetostriction of $Fe_{81}Ga_{19}$ by approaching an instable phase boundary, Scripta Mater. 146 (2018) 200–203.
[23] Y.K. He, C.B. Jiang, W. Wu, B. Wang, H.P. Duan, H. Wang, T.L. Zhang, J.M. Wang, J.H. Liu, Z.L. Zhang, P. Stamenov, J.M.D. Coey, H.B. Xu, Giant heterogeneous

magnetostriction in Fe–Ga alloys: effect of trace element doping, Acta Mater. 109 (2016) 177–186.
[24] A.G. Khachaturyan, D.V. iehland, Structurally heterogeneous model of extrinsic magnetostriction for Fe-Ga and similar magnetic alloys: Part I. Decomposition and confined displacive transformation, Metall. Mater. Trans. A 38 (13) (2007) 2308–2316.
[25] A.G. Khachaturyan, D.V. iehland, Structurally heterogeneous model of extrinsic magnetostriction for Fe-Ga and similar magnetic alloys: Part II. Giant magnetostriction and elastic softening, Metall. Mater. Trans. A 38 (13) (2007) 2317–2328.